Heating of solar chromosphere by electromagnetic wave absorption in a plasma slab model

D. Tsiklauri and R. Pechhacker

Astronomy Unit, School of Mathematical Sciences, Queen Mary University of London,
Mile End Road, London, E1 4NS, United Kingdom
(Dated: April 14, 2011)

The heating of solar chromospheric inter-network regions by means of the absorption of electromagnetic (EM) waves that originate from the photospheric blackbody radiation is studied in the framework of a plasma slab model. The absorption is provided by the electron-neutral collisions in which electrons oscillate in the EM wave field and electron-neutral collisions damp the EM wave. Given the uncertain nature of the collision cross-section due to the plasma micro-turbulence, it is shown that for plausible physical parameters, the heating flux produced by the absorption of EM waves in the chromosphere is between $20-45$ % of the chromospheric radiative loss flux requirement. It is also established that there is an optimal value for the collision cross-section, 5×10^{-18} m^2, that produces the maximal heating flux of 1990 W m^{-2}.

I. INTRODUCTION

The problem of heating of the solar atmosphere, the sharp temperature raise from photospheric 6000K to few 10^6K in the corona has been a long standing problem of solar physics. There is no lack of possible heating mechanisms in the *corona* with the two main candidates being so-called direct current (DC) models that are based on the magnetic reconnection and alternating current (AC) models that are based on magnetohydrodynamic (MHD) wave dissipation [1], alongside with few dozen other, less widely accepted [2, 3] or less successful ones [4]. In the *chromosphere*, however, until recently, a general agreement was that it is heated by the absorption of the acoustic waves. A distinction needs to be drawn between wave heating of different parts of the chromosphere. The chromosphere of the quiet Sun can be broadly split into two parts: (i) the magnetic network, which marks the boundaries in between the super-granulation cells; and (ii) the inter-network regions, which constitute the bulk surface area of the chromosphere (i.e. the super-granulation cell interiors).

In the magnetic network the magnetic field is nearly radial (vertical) and quite strong (of the order of few kG). Since the strong magnetic field there provides a substantial amount of free energy, in principle it seems reasonable to believe that the magnetic network can be heated by the dissipation of MHD waves [5]. However, the role of magnetic reconnection in the heating of the magnetic network cannot be discounted. For example, there seems to be an evidence of forced magnetic reconnection taking place in the photosphere [6], as well as in chromosphere [7]. The estimates of the heating flux produced by plausible reconnection models seem to fall short by up to two orders of magnitude from the quiet chromosphere and coronal heating requirements [8]. At the same time Ref.[5] and other similar works, that base their conclusions on the numerical simulation results, do not make precise predictions for the heating rates produced by the dissipation of MHD waves in the chromospheric magnetic network.

The situation with the heating of inter-network regions where magnetic fields are weak is even worse than with the magnetic network. On one hand, this is because of the lack of the magnetic energy. On the other hand, the results of Ref.[9] indicate that the acoustic energy flux of the high-frequency (10-50mHz) acoustic waves (that were previously believed to constitute the dominant heating mechanism of the chromosphere) falls short, by a factor of at least ten, to balance the radiative losses in the solar chromosphere. This led them to a conclusion that the acoustic waves cannot constitute the dominant heating mechanism of the solar chromosphere. This conclusion has been challenged by Ref.[10], who suggests that the observations reported by Ref.[9] only detect 10% of the acoustic wave flux perhaps because of the limited spatial resolution. Ref.[11] report somewhat higher than usual flux carried by the acoustic waves at photospheric heights (250 km) as well as compile a useful list of up to date acoustic heating flux measurements.

In this context, in this paper we explore an alternative to the acoustic wave heating idea of the quiet chromosphere. In particular, we investigate the following proposition:

(i) It is known that the solar irradiance spectrum, that comes out of photosphere, is well approximated by an effective blackbody at a temperature of $T = 5762$ K, in the frequency range of $f = 30-1667$ THz (corresponding to the wavelengths range of $10-0.18\ \mu$m) (see e.g. Figure 2.3 from Ref.[1]). Therefore, we assume that the radiative heating flux with the Planckian brightness distribution as a function of frequency penetrates the lower part of the solar atmosphere (photosphere, $h = 0 - 500$ km and chromosphere, $h = 500 - 2200$ km).

(ii) Instead of solving radiative transfer equations, we take the photospheric blackbody flux of $T = 5762$ K, and quantify how much electromagnetic (EM) radiative flux is absorbed using a plausible model for EM

wave absorption, which is based on Ref.[12] plasma slab model combined with the VAL-C model of chromosphere [13]. Ref.[12] plasma slab model is based on splitting a smoothly varying, non-uniform density, weakly ionised plasma with the uniform magnetic field along the density gradient, into a set of thin sub-slabs with a uniform density in each sub-slab - thus providing a discretized version of the smooth density profile. The absorption of the EM radiation is based on two physical effects: electron-neutral collisions and electron cyclotron resonance. For the considered in our model radial magnetic field value of 0.2 kG, electron cyclotron frequency is $f_{ce} = eB/2\pi m_e = 0.00056$ THz. Also, for the considered model parameters, the ratio of electron-neutral collision frequency and electron cyclotron frequency, $\nu_{en}/f_{ce} << 1$, which ensures that the collisions would not affect any electron cyclotron resonance damping. Therefore EM wave absorption via electron cyclotron resonance is negligibly small in the considered range of frequencies $2 - 2000$ THz. We refer the interested reader to Ref.[12] for the details of the plasma slab model. However, we re-iterate the key points of the model in Section 2.

As a result we find that for plausible physical parameters, the heating flux produced by the absorption of EM waves in the chromosphere is between $20 - 45$ % of the VAL-C radiative loss flux requirement. We also establish that there is an optimal value for the collision cross-section, 5×10^{-18} m^2, that produces the maximal heating flux of 1990 W m^{-2}.

The paper is organised as follows: In Section 2 we describe the model. In Section 3 we present the numerical results and we close with the Conclusions in Section 4.

II. THE MODEL

The interaction of EM wave with a plasma slab has been a subject of a number of studies see e.g. Ref.[12], references therein, and a more recent work [14].

Following the general approach of Ref.[12], we consider a slab that contains 22 sub-slabs each having thickness of 100 km. In each sub-slab density and temperature are assumed to be uniform, but these vary as we go from one slab to the next. This variation is prescribed by the VAL-C model [13]. This way, in the first slab, that corresponds to the 50 km above photospheric level, we have temperature of T=5840 K, neutral hydrogen number density $n_H = 9.203 \times 10^{22}$ m^{-3}, electron number density of $n_e = 2.122 \times 10^{19}$ m^{-3}. In the final 22nd slab, that corresponds to the 2200 km above photospheric level the plasma parameters are T=24000 K, $n_H = 1.932 \times 10^{16}$ m^{-3}, $n_e = 2.009 \times 10^{16}$ m^{-3}. In between these values we use linear interpolation for the thermodynamic parameters. The uniform magnetic field with $B = 0.02$ T (0.2 kG) is directed through all sub-slabs in the vertical (radial) direction. We use a relatively small value of B that is commensurate with the chromospheric inter-network regions. However, we note that the model outcomes (such

as e.g. the resultant EM wave absorption) depend weakly on the magnetic field value used (at least in the plausible range of variation of the field in the chromosphere). Also the fact that the magnetic field is vertical describes the quiet Sun reasonably well. Ref.[15] found no evidence for any predominance of horizontal fields on the quiet Sun. They find that (i) the angular distribution of the field varies steeply with flux density. (ii) For the largest flux densities the distribution is extremely peaked around the vertical direction. (iii) For the smaller vertical flux densities the distribution widens to become asymptotically isotropic in the limit of zero flux density. The apparent dominance of horizontal fields for flux densities below 5 G is shown to be an artifact of noise.

Our representation of the number density and temperature variation in the photosphere and chromosphere by means of uniform sub-slabs is valid when the variation over height is slow. This is indeed the case in the photosphere and chromosphere (we exclude the transition region and corona from our consideration also on the grounds that the dispersion relation that we use below is applicable for *weakly* ionised plasma). The expression for the complex dielectric constant for the weakly ionised, magnetised plasma with the angle between the propagation direction of the incident EM wave and the magnetic field B, $\theta = 0$ is taken from Ref.[12]:

$$\tilde{\varepsilon}_r = 1 - \frac{\omega_{pe}^2/\omega^2}{[1 - i\nu_{en}/\omega] \pm \omega_{ce}/\omega}. \tag{1}$$

Here $\omega_{pe} = \sqrt{n_e e^2/(\varepsilon_0 m_e)}$, $\omega_{ce} = eB/m_e$ and ν_{en} (see Eq.(7) below for the definition) are the electron plasma frequency, electron cyclotron angular frequency and electron-neutral collision frequency, respectively. The angular frequency ω of the EM harmonic is related to the frequency, f, in the usual way $\omega = 2\pi f$. The sign $\pm$ refers to the left- and right-hand polarisation of the EM wave and i is the imaginary unit. The EM wave reflection coefficient at the $(k+1)$th sub-slab interface is given by

$$\Gamma(k+1) = \frac{\sqrt{\tilde{\varepsilon}_r(k)} - \sqrt{\tilde{\varepsilon}_r(k+1)}}{\sqrt{\tilde{\varepsilon}_r(k)} + \sqrt{\tilde{\varepsilon}_r(k+1)}}. \tag{2}$$

One can calculate the reflected and transmitted power, P_r and P_t, respectively, using formulae:

$$P_r(f) = P_i(f)\left[|\Gamma(1)|^2 + \right.$$
$$\left. \sum_{j=2}^{22}\left(|\Gamma(j)|^2 \prod_{i=1}^{j-1}\left[e^{-4\alpha(i)d}\left(1 - |\Gamma(i)|^2\right)\right]\right)\right] \tag{3}$$

$$P_t(f) = P_i(f)\prod_{i=1}^{22}\left[e^{-2\alpha(i)d}\left(1 - |\Gamma(i)|^2\right)\right], \tag{4}$$

where P_i is the incident EM wave power, d is the sub-slab thickness and $\alpha(i)$ is the real part of the complex

propagation constant of a plane wave in a magnetised plasma corresponding to slab i

$$\alpha(i) = \frac{\omega}{c}\text{Re}\left[\sqrt{-\tilde{\varepsilon}_r(i)}\right] = \frac{\omega}{c}\sqrt{\frac{|\tilde{\varepsilon}_r(i)| - \text{Re}[\tilde{\varepsilon}_r(i)]}{2}}. \quad (5)$$

Note that Eqs.(1)-(4) are identical to the corresponding equations from Ref.[12]. As in Ref.[12] we neglect the effect of multiple reflections of waves, i.e. each wave gets reflected at a maximum of one slab interface, however may be absorbed in any location.

The total absorbed power, P_a is then given by

$$P_a(f) = P_i(f) - P_r(f) - P_t(f). \quad (6)$$

Note that for $\theta = 0$ the above expressions for the reflection, transmission and absorption coefficients are independent of the EM wave polarisation, except for the $\pm$ sign in Eq.(1) for the left- and right-hand polarisation of the EM wave (see e.g. Ref.[16], pp. 71-94). A simple numerical code was written to calculate the above absorbed, reflected and transmitted EM power. We have tested the code by successfully reproducing Figures 1-9 from Ref.[12], using their set of physical parameters.

The above formulae contain the electron-neutral collision frequency ν_{en}. For the latter we use the standard expression from Ref.[17], p.39,

$$\nu_{en} = n_0\sigma\sqrt{kT_e/m_e}, \quad (7)$$

where n_0 is the neutral number density, σ is the collision cross-section and the square root is essentially the electron thermal speed. For n_0 we use values of neutral hydrogen number density n_H in each sub-slab, and for T_e we use the temperature T; both according to the VAL-C model. Thus, in each presented numerical model run we regard σ as fixed. However, since ν_{en} is a function of density and temperature, each sub-slab has its own set value.

In order to calculate the absorbed EM flux we use equal $1/2$ statistical weights of the left- and right-hand polarised EM wave total absorbed powers $P_{a,L}$ and $P_{a,R}$ as following

$$P_a(f) = \frac{1}{2}P_{a,L}(f) + \frac{1}{2}P_{a,R}(f). \quad (8)$$

Thus, the total absorbed EM flux can be calculated using the following integral

$$F_a[\text{Wm}^2] = \pi \int_{f_{\min}}^{f_{\max}} A(f)B_f(f)df, \quad (9)$$

where $B_f(f)$ is the Planck function $B_f(f) = 2hf^3/\left[c^2(\exp[hf/(kT)] - 1)\right]$ and $A(f)$ is the total absorption coefficient as a function of frequency given by the following expression
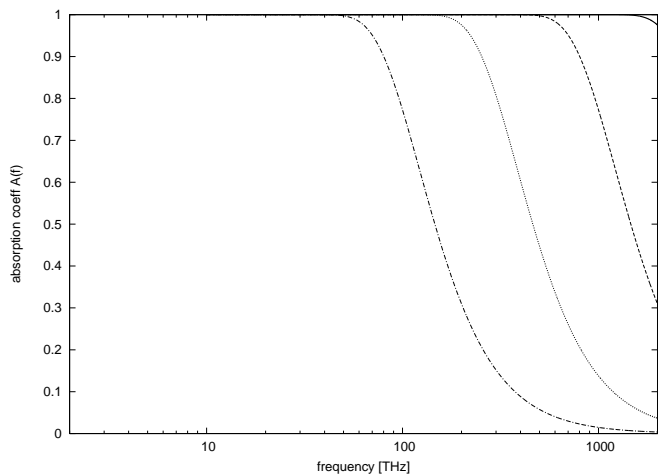
$$P_a(f) = P_i(f)A(f). \quad (10)$$

FIG. 1: Absorption coefficient $A(f)$ is a function of EM wave frequency f for different values of the cross-section σ. Solid line corresponds to $\sigma = 5 \times 10^{-16}$, dashed $\sigma = 5 \times 10^{-17}$, dotted $\sigma = 5 \times 10^{-18}$, dot-dashed $\sigma = 5 \times 10^{-19}$.

III. RESULTS

The dissipation coefficients in the solar atmosphere are not known precisely. There are good reasons to believe that the dissipation coefficients, such as resistivity and viscosity, which in turn depend on plasma species mutual collision cross-sections and collision frequencies (including ν_{en}), have so-called "anomalous" values. The "anomaly" is in the sense of their departure (mostly increase) from the classical (laminar) plasma transport theory values. It is believed that the anomalous dissipation coefficients result from the plasma micro-turbulence. The latter provides additional centres of scattering for the plasma particles in addition to their mutual collisions. In effect this means that in Eq.(7) we should use $\sigma = \sigma_{en} + \sigma_{turbulent}$, i.e. the effective anomalous cross-section is a sum of usual electron-neutral and turbulent plasma cross-sections. Note that $\sigma_{en} \approx 5 \times 10^{-19}$ m^2 and is weakly dependent on temperature [17]. Little is known about the $\sigma_{turbulent}$ apart from it can be orders of magnitude larger than σ_{en}. Since the theory of plasma micro-turbulence is not complete, we simply vary the collision cross-section σ in Eq.(7) by a few orders of magnitude, in order to study the effects of anomalous dissipation coefficients on the quiet chromosphere heating. We start presentation of the results by plotting, in Figure 1, the EM wave absorption coefficient, $A(f)$, as a function of frequency for various values of σ. The considered frequency range is commensurate with the range $f = 30 - 1667$ THz where the solar irradiance spectrum, that comes out of photosphere, is well approximated by an effective blackbody at $T = 5762$ K (see e.g. Figure 2.3 from Ref.[1]).

We gather from Figure 1 that (i) a decrease in σ generally results in an overall reduction of the absorption coefficient; and (ii) different frequencies are absorbed dif-
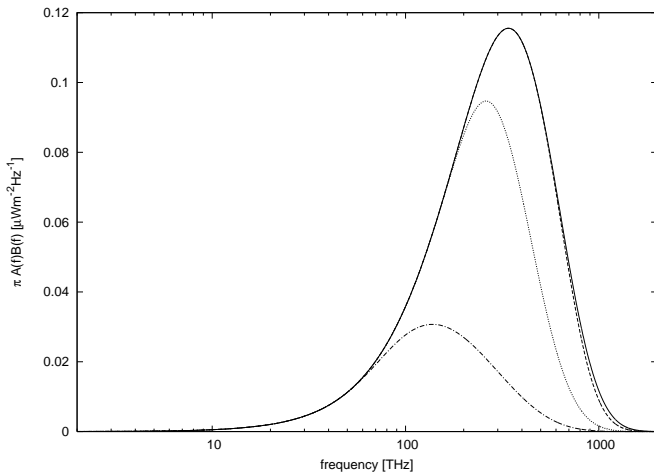
FIG. 2: The absorbed EM flux density, $\pi A(f)B_f(f)$, as a function of frequency for various values of σ. Solid line corresponds to $\sigma = 5 \times 10^{-16}$, dashed $\sigma = 5 \times 10^{-17}$, dotted $\sigma = 5 \times 10^{-18}$, dot-dashed $\sigma = 5 \times 10^{-19}$.

FIG. 3: The heating rate for the different values of σ as a function of height above photosphere. The VAL-C empirical model (solid); the next four curves are calculated using Eq.(11): $\sigma = 5 \times 10^{-17}$ (long-dashed), $\sigma = 5 \times 10^{-18}$ (dotted), $\sigma = 5 \times 10^{-19}$ (dot-dashed), $\sigma = 5 \times 10^{-20}$ (short-dashed).

ferently - high frequencies show weaker absorption than low ones. As to the observation (i), the explanation can be provided by analysing by Eqs. (1) - (4). It is clear from Eqs. (3) and (4) that the electron-neutral collision frequency ν_{en} provides the only dissipation effect. The exponential factor $e^{-\alpha d}$ dominates the heat flux absorption. For the considered model parameter range, it can be shown by calculating $\partial \alpha / \partial \nu_{en}$ derivative numerically that $\partial \alpha / \partial \nu_{en} > 0$. Therefore one can deduce that the heat flux absorption decreases with the decrease in cross-section. As to the observation (ii), a possible physical explanation could be that when the frequency of the EM radiation is increased, electrons due to their small but finite inertia do not have time to catch up with (i.e. couple to) the EM wave. Hence the EM wave frequency increase results in a decrease of the absorption coefficient.

In Figure 2 we show the behaviour of the integrand of Eq.(9), $\pi A(f)B_f(f)$, which has a physical meaning of the absorbed EM flux density (i.e. flux per unit frequency) as a function of frequency for various values of σ. We observe that due to the frequency dependence of $B_f(f)$ that has a peak, the absorbed EM flux density is also peaked. The two conclusions that follow are: the decrease in the cross-section results in (i) the overall reduction of the the absorbed EM flux density; and (ii) shift of the absorbed EM flux density's peak towards the smaller frequencies.

Next we calculate the volumetric heating rate produced by the absorption of the EM waves. Above we have presented the behaviour of the total absorption coefficient and the absorbed EM flux density for the full set of 22 slabs as a function of frequency. We obtained the expression for the total absorbed flux by integrating over the relevant interval of frequencies using Eq.(9). In order to obtain the distribution of the absorbed EM energy as a function of height, we perform a numerical differentiation of the calculated total absorbed flux values. The
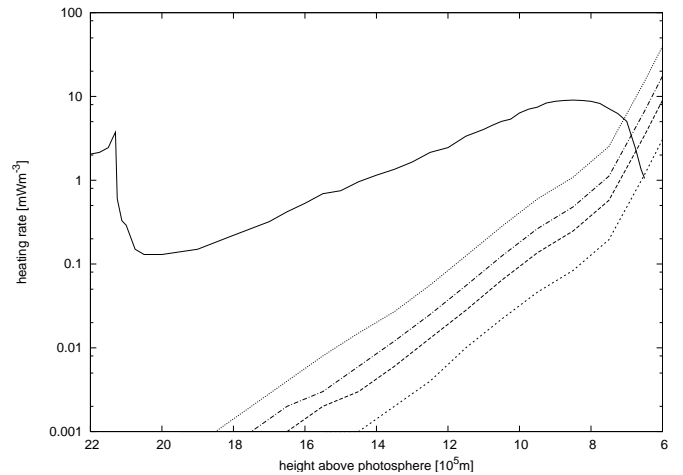
differentiation yields the heating rate $H(k)$ in slab k,

$$H(k) = \frac{F_a(k) - F_a(k-1)}{d} \qquad (11)$$

where the $F_a(k)$ are calculated by ignoring the existence of slabs above slab number k.

In Figure 3 we plot the heating rate for the different values of σ as a function of height above photosphere. Clearly, the model predictions for the heating rate fall short in matching the empirical radiative loss calculated by the VAL-C model of the chromosphere. We gather that (i) the heating rate decreases rapidly with height; and (ii) in the region of 500 km - 2200 km above photosphere there is an optimal value for σ that produces a maximal heating rate. The latter is evidenced by the fact that $\sigma = 5 \times 10^{-18}$ (dotted) curve is above the both $\sigma = 5 \times 10^{-17}$ (long-dashed) and $\sigma = 5 \times 10^{-19}$ (dot-dashed) curves. Note that the model predictions for the heating rate presented in Figure 3 underestimate the actual heating rate produced by the absorption of EM waves. This is due to the following reasons: (i) an error introduced by the numerical differentiation with respect to height (it is known that the numerical differentiation always introduces the numerical diffusion); and (ii) ignoring the contribution to the absorption due to reflected waves. The former is unavoidable, while the latter can be regarded as a shortcoming of our heating rate calculation. Our motivation for calculating the (volumetric) heating rate as a function of height was to compare our model predictions to the results of VAL-C empirical radiative cooling rate (see their Figure 49). Naturally, we can improve our calculation by *directly* calculating the total heating flux of the chromosphere. We do this by applying Eq.(9) for all 22 sub-slabs that cover entire the photosphere and chromosphere (heights of $0 - 2200$ km)

and then subtracting contribution from the first 5 photospheric sub-slabs $(0-500$ km$)$, because we are concerned only with the chromosphere. Such *heating flux* [W m^{-2}] calculation is free from the above two sources of the underestimation that arose in the calculation of the *(volumetric) heating rate* [W m^{-3}]. Further, the most exact calculation of the total absorbed EM flux is as follows:

In order to extract the total absorbed flux of a slab interval $[a; b]$, we have to account for the possibility of waves being reflected at an interface higher up than slab b and being absorbed within the interval on their way back. In the following we will use the notation $A|_a^b$ for the absorption coefficient of a plasma slab bounded by slabs number a and b, both included in the interval. Further we define

$$A|_a^b = 1 - R|_a^b - T|_a^b \qquad (12)$$

where $R|_a^b$ and $T|_a^b$ represent reflection and transmission coefficients of the interval and can be calculated by Eq.(3)-(4). At this point we stress that by using Eq.(3)-(4) we neglect the effect of multiple reflections of waves, meaning that each wave gets reflected at a maximum of one slab interface, however may be absorbed in any location. Further we define that only coefficients that follow $1 \le a \le b \le N$, where N is the total number of slabs, are non-zero. First we consider the case $a = 1$ and b arbitrary. We write for the absorption coefficient

$$A|_1^b = A|_1^N - A|_{b+1}^N T|_1^b \qquad (13)$$

where the last term on the right hand side accounts for absorption of waves within layers higher up than slab b that have passed through the interval. Extending the formalism to arbitrary a it holds true that

$$A|_a^b = A|_1^N - A|_{b+1}^N T|_1^b - A|_1^{a-1} - T|_1^{a-1} R|_a^N (A|_1^{a-1})^* \quad (14)$$

where

$$(A|_1^{a-1})^* = 1 - T|_1^{a-1} = 1 - \prod_{i=1}^{a-1} \left[e^{-2\alpha(i)d} \right]. \qquad (15)$$

The factor $(A|_1^{a-1})^*$ accounts for the absorbed radiation within the interval $[1; a-1]$ but neglects the multiple reflections. We gather from Eq.(14) that we have added a term that gives absorptions at layers lower than a and another term that accounts for waves that have initially been transmitted through those lower layers, then get reflected at higher levels and absorbed below level a on their way back down.

The results of the these calculations, inserting $N = 22$, $a = 6$ and $b = 22$, are shown in Figure 4, where we plot the total absorbed EM flux as a function of σ. We gather from Figure 4 that (i) there is an optimal value for $\sigma = 5 \times 10^{-18}$ m^2 that produces the maximal heating flux of 1990 W m^{-2}. The latter is about 45 % of the chromospheric radiative losses; (ii) For the value of $\sigma = 5 \times 10^{-19}$ m^2 that is predicted by the classical (laminar) plasma transport theory [17], which ignores contribution from the plasma-microturbulent transport, the
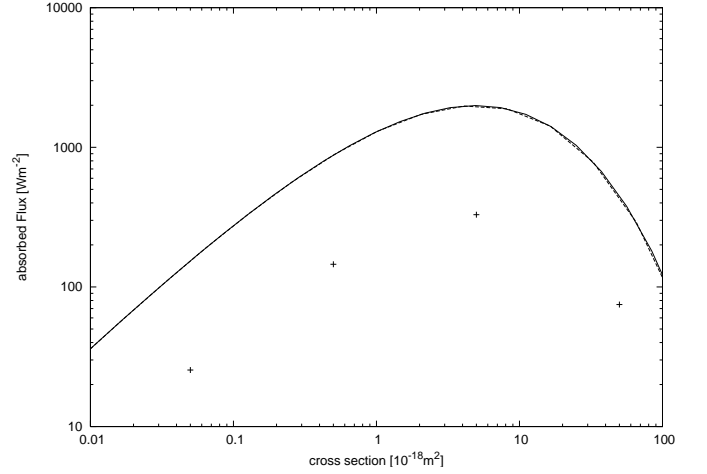

FIG. 4: The total absorbed EM flux as a function of σ. The solid curve corresponds to the precise calculation according to Eq.(14). The dashed curve corresponds to the the calculation by applying Eq.(9) for all 22 sub-slabs that cover entire photosphere and chromosphere (heights of $0-2200$ km) and then subtracting the contribution from the first 5 photospheric sub-slabs $(0-500$ km$)$. Four crosses correspond to the area under the long-dashed, dotted, dot-dashed and short-dashed curves in Figure 3 that cover chromospheric heights between 6th and the 22nd sub-slabs $500-2200$ km.

total heating flux by the absorption of EM waves in the chromosphere our model predicts 880 W m^{-2}. Which is only 20% percent of the heating flux requirement of 4280 W m^{-2} [13]. Since precise value of σ is unknown due to a lack of the detailed plasma-microturbulent transport theory, we conclude that the actual heating flux produced by the absorption of EM waves in the chromosphere is between $20-45$ % of the VAL-C radiative loss flux requirement. Note that the behaviour described in Figure 4 that the heating flux has a maximum when plotted as a function of cross-section σ is true when only chromospheric sub-slabs $6-22$ are considered (i.e. when contribution from the photospheric sub-slabs $1-5$ is not included). We also remark that the difference between the solid curve that corresponds to the precise calculation according to Eq.(14) and the dashed curve that corresponds to the the calculation by applying Eq.(9) for all 22 sub-slabs that cover entire photosphere and chromosphere (heights of $0-2200$ km) and then subtracting the contribution from the first 5 photospheric sub-slabs $(0-500$ km$)$ is rather small and barely distinguishable to the plotting accuracy. The close overlap of the two curves is an indication of the last term in Eq.(14) being negligibly small. This term accounts for the radiation that is initially transmitted into slabs 6 and higher, reflected somewhere in the higher slabs and then again absorbed within the slabs 1-5. It is clear from Fig. 3 that the absorption in the lower layers is higher compared to the upper ones. Hence, the last term in Eq.(14) will not make a considerable contribution when the reflection and transmission coefficients $R|_a^N$ and $T|_1^{a-1}$ are sufficiently

small, such that the overall product $T|_1^{a-1}R|_a^N(A|_1^{a-1})^*$ is negligible. For for the chromospheric parameters the last term in Eq.(14) is negligibly small, thus the plotted curves in figure 4 are barely distinguishable.

IV. CONCLUSIONS

In this paper we put to test a simple proposition that some of the problems of the chromospheric inter-network regions (regions with weak magnetic field which constitute the bulk of solar chromosphere surface), discussed in the Introduction section can be alleviated by inclusion of the absorption of photospheric EM radiation in the plasma sub-slab based model.

On one hand, we know that that the solar irradiance spectrum, that comes out of photosphere, is well approximated by an effective blackbody at a temperature of $T = 5762$ K, in the frequency range of $f = 30 - 1667$ THz. Therefore, we can assume that the radiative heating flux with the Planckian brightness distribution as a function of frequency illuminates lower part of the solar atmosphere (photosphere, $h = 0 - 500$ km and chromosphere, $h = 500 - 2200$ km).

On the other hand, instead of solving radiative transfer equations, we can take photospheric blackbody flux of $T = 5762$ K, and quantify how much electromagnetic (EM) radiative flux is absorbed using a plausible model for the EM wave absorption which is based on Ref.[12] plasma slab model combined with VAL-C model of chromosphere [13]. Our model is based on splitting a weakly ionised plasma slab with the uniform magnetic field along a smooth density gradient, into a set of narrow sub-slabs with a uniform density in each slab - hence providing a discretized version of the smooth density gradient. In the relevant frequency range $(2-2000$ THz), the absorption of the EM radiation is due to the electron-neutral collisions, while the electron cyclotron resonance can be ignored. The absorption of the EM radiation due to the electron-neutral collisions happens because the electrons oscillate in the EM wave field and electron-neutral collisions (i.e. their mutual friction) then results in the damping of the EM wave.

We also include a contribution to the cross-section from the anomalous plasma micro-turbulence, which we incorporate in an additive way.

Our model has two potential weaknesses: (i) to what extent the radiative heating flux of the photosphere deviates from the Planckian brightness distribution as a function of frequency? and (ii) whether the *absorption* of EM radiation can be described by the plasma sub-slab model which assumes local thermodynamic equilibrium (LTE)? Concerning the first question we state that it is well known that the solar irradiance spectrum, that comes out of photosphere, is well approximated by an effective blackbody at a temperature of $T = 5762$ K, in the frequency range of $f = 30 - 1667$ THz. Also, there are plausible models of solar photosphere that use LTE

assumption (see e.g. Ref.[18]) that implies the applicability of the Planckian brightness function. As to the second question we remark that indeed in order to properly work out the chromospheric (radiative) *losses*, one needs to consider non-LTE effects. Strong radiation field in the chromosphere can drastically alter the occupation numbers of the energy levels in atoms, thus producing non-LTE net radiative loss [19]. We assert, however, that the chromospheric *heating* process can be regarded as an LTE process, given the *steady* inflow of EM radiation from the photosphere. After all, the chromospheric heating models that are based on the absorption of acoustic shock wave energy use equations of hydrodynamics which imply LTE, and it is only the radiative *losses* that are treated by the non-LTE radiative transport as in e.g. Ref.[9].

As a result we find that:

(i) for plausible physical parameters, the heating flux produced by the absorption of EM waves in the chromosphere is between $20-45$ % of the VAL-C model radiative loss flux requirement. The variation range is because of the uncertainties in the collision cross-section due to the plasma micro-turbulence.

(ii) We also established that for absorption in the region 500 km - 2200 km above photosphere there is an optimal value for $\sigma = 5 \times 10^{-18}$ m^2 that produces the maximal heating flux of 1990 W m^{-2}.

From the observational point of view, if the absorption of EM waves in the frequency range $2 - 2000$ THz has a significant role to play in the heating of quiet chromosphere, as suggested by our findings, then the plasma slab model also predicts that:

(i) There is a good case for the electron-neutral anomalous collision cross-section to be a factor of 10 larger than the value predicted by the classical plasma transport. Ref.[20] presented plasma resistivity (which is proportional to both the collision frequency and cross-section) measurements in the reconnection current sheet of the Magnetic Reconnection Experiment. They established that in some regimes, the measured resistivity values can be more than an order of magnitude larger than the classical Spitzer value. Therefore it would seem likely that the collision cross-section in the chromosphere would also assume some anomalous value.

(ii) There should be a good correlation of the total solar irradiance with the Mg-index (which represents the chromospheric excess radiation relative to the photosphere) on a long-term (1 month or more) timescale. This is because our model takes photospheric blackbody EM wave flux as the source of energy, that irradiates chromosphere from below (a torch shining from the below analogy is relevant here). In fact, this is exactly what is observed: Ref.[21] presents the data that shows that the total solar irradiance and the Mg-index have a correlation coefficient of 0.8 using monthly data averages (see their Figure 1 and pertinent discussion). The correlation is somewhat worse of a shorter timescales, e.g. daily data averages – this has a good explanation in that contribution from the solar

features such as sunspots and faculae (that affect photospheric total solar irradiance) and plages (that affect chromospheric brightness and are in fact mapped closely to the faculae below) average out on the long timescales and generally track to solar activity cycle (that has a proxy of number of sunspots).

(iii) Unlike in the photosphere, the chromospheric brightness should not decrease with the increase of the magnetic field. This is because in our model EM wave absorption depends on the magnetic field rather weakly. This is also what is observed: Ref.[22] find that CaII K line core contrast (the relative difference between the intensity at a given magnetogram and the quiet Sun intensity) that is a measure of chromospheric brightness is weakly increasing with the magnetic field as $\propto B^{0.6}$. In the photosphere the contrast of a continuum in the green part of the solar spectrum initially increases with B up to 0.02 Tesla but then sharply decreases with B above 0.05 Tesla. Ref.[21] explain chromospheric rise of brightness with the increase of magnetic field for small B's (0.01 T) is due to the density increase of the magnetic flux tubes, and for large B's (> 0.05T) subsequent slower rise is due to the quenching of the wave activity. As Ref.[23] have shown, the strong magnetic fields inhibit average horizontal flow speeds in the granules.

Thus in conclusion the plasma slab model predictions seem also to conform with the available observational data.

[1] M. J. Aschwanden, *Physics of the Solar Corona. An Introduction with Problems and Solutions (2nd edition)* (Chichester, UK: Praxis Publishing Ltd, 2005).

[2] J. D. Scudder, Astrophys. J. **427**, 446 (1994).

[3] D. Tsiklauri, Astron. Astrophys. **455**, 1073 (2006).

[4] D. Tsiklauri, Astron. Astrophys. **441**, 1177 (2005).

[5] S. S. Hasan and A. A. van Ballegooijen, Astrophys. J. **680**, 1542 (2008).

[6] D. B. Jess, M. Mathioudakis, P. K. Browning, P. J. Crockett, and F. P. Keenan, Astrophys. J. **712**, L111 (2010).

[7] J. Chae, P. R. Goode, K. Ahn, V. Yurchysyn, V. Abramenko, A. Andic, W. Cao, and Y. D. Park, Astrophys. J. **713**, L6 (2010).

[8] D. W. Longcope and C. C. Kankelborg, Astrophys. J. **524**, 483 (1999).

[9] A. Fossum and M. Carlsson, Nature (London) **435**, 919 (2005).

[10] W. Kalkofen, J. Astrophys. Astron. **29**, 163 (2008).

[11] N. Bello González, M. Franz, V. Martínez Pillet, J. A. Bonet, S. K. Solanki, J. C. del Toro Iniesta, W. Schmidt, A. Gandorfer, V. Domingo, P. Barthol, et al., Astrophys. J. **723**, L134 (2010).

[12] D. L. Tang, A. P. Sun, X. M. Qiu, and P. K. Chu, IEEE Transactions on Plasma Science **31**, 405 (2003).

[13] J. E. Vernazza, E. H. Avrett, and R. Loeser, Astrophys. J. Supl. Ser. **45**, 635 (1981).

[14] C. Yuan, Z. Zhou, X. Xiang, H. Sun, and S. Pu, Physics of Plasmas **17**, 113304 (pages 7) (2010).

[15] J. O. Stenflo, Astron. Astrophys. **517**, A37+ (2010).

[16] M. A. Heald and C. B. Wharton, *Plasma Diagnostics With Microwaves* (New York: Krieger, 1978).

[17] J. D. Huba, *NRL Plasma Formulary* (Washington DC: Naval Research Laboratory, 2009).

[18] B. Gustafsson, B. Edvardsson, K. Eriksson, U. G. Jørgensen, Å. Nordlund, and B. Plez, Astron. Astrophys. **486**, 951 (2008).

[19] D. Mihalas, *Stellar atmospheres /2nd edition/* (San Francisco: W. H. Freeman and Co., 1978).

[20] F. Trintchouk, M. Yamada, H. Ji, R. M. Kulsrud, and T. A. Carter, Physics of Plasmas **10**, 319 (2003).

[21] S. K. Solanki, in *The Physics of Chromospheric Plasmas*, edited by P. Heinzel, I. Dorotovič, & R. J. Rutten (2007), vol. 368 of *Astronomical Society of the Pacific Conference Series*, pp. 481–+.

[22] C. J. Schrijver, J. Cote, C. Zwaan, and S. H. Saar, Astrophys. J. **337**, 964 (1989).

[23] A. M. Title, T. D. Tarbell, K. P. Topka, S. H. Ferguson, R. A. Shine, and SOUP Team, Astrophys. J. **336**, 475 (1989).